Appl. Phys. 2, 247—256 (1973)

Applied Physics

Ionized Impurity Scattering in Degenerate In_2O_3

Robert Clanget

Experimentalphysik, Universität des Saarlandes,
D-6600 Saarbrücken, Fed. Rep. Germany

Received 22 June 1973/Revised 10 August 1973

Abstract. Thin films of In_2O_3 are prepared by the spraying method. The concentration of charge carriers is changed from about 8×10^{19} cm^{-3} to 5×10^{20} cm^{-3} by suitable doping with Sn. The optical effective mass is found to depend slightly on carrier concentration. Electrical and optical measurements indicate that electrons are scattered predominantly by charged impurity centres. Structural investigations show that grain boundary scattering can be neglected. The interpretation of the experimental results is mainly based on a paper by von Baltz and Escher, where analytical formulas for the imaginary part of the complex dielectric constant are given for the most important scattering mechanisms in (degenerate) semiconductors.

Index Headings: Ionized impurity scattering — In_2O_3-films

A variety of papers deals with the electrical and optical properties of *n*-type In_2O_3 as single crystals or thin films, the latter being prepared by sputtering in an appropriate atmosphere or by spraying suitable solutions of organic or inorganic In-compounds onto pre-heated substrates like glass or fused quartz [1–15]. The films if sprayed or sputtered are exclusively *n*-type and show degeneracy at a carrier concentration of about 10^{19}cm^{-3}. They have a polycristalline structure and adhere to the substrate very well.

In undoped samples the carrier concentration is due to indium excess or oxygen deficiency and can be changed by a reducing heat treatment [6; 7]. Doping with a metal of higher valency like Sn may lead to such a high carrier density as 10^{21}cm^{-3} [15].

The electron mobility reported usually varies between 10 cm^2/Vs and 60 cm^2/Vs. An unusually high value (170 cm^2/Vs) was measured by Groth [5] on Zr-doped samples.

The optical properties reflect the properties of a free electron gas imbedded in a medium of dielectric constant ε_g, where ε_g is due to core polarisation.

Thin films are highly transmittant in the visible part of the spectrum and show increasing absorption at longer wavelengths. Coupled with the decreasing transmissivity is an increase in reflectivity, where the more or less sharp onset (depending on film thickness and electron mobility) occurs in the vicinity of the plasma frequency ω_p defined by

$$\omega_p^2 = Ne^2/(\varepsilon_0 \varepsilon_g m_{\text{opt}}), \tag{1}$$

N being the carrier concentration, e the electron charge, ε_0 the permittivity of vacuum, ε_g the optical dielectric constant mentioned above, and m_{opt} the optical effective mass.

Regarding the scattering mechanism of electrons in In_2O_3 contradictory interpretations exist. From measurements of the Seebeck-effect Fistul' and Vainshtein [13] concluded that acoustical phonon scattering is the main scattering process. Groth [5] supposed that structural effects are responsible for limiting the mobility. Finally Müller [6; 7] infered that scattering at ionized impurities predominates.

This paper attempts to underline the assumption that ionized impurity scattering is the most effective mechanism determining the electrical and optical properties of thin, highly conductive In_2O_3-films. At the same time, it is interesting to compare the optical properties of a degenerate semiconductor with the new theoretical results of von Baltz and Escher [16].

1. Experimental Procedure

The films were prepared by spraying solutions of $InCl_3$ in buthylacetate (samples S 7 and S 8) or indiumacetylacetonate in *N,N*-dimethylformamid as a fine mist onto hot plates (600° C) of fused quartz (Infrasil). The doping compound is dibutyltinoxide dissolved in the solution of the In compound. The proportion of Sn amounts to only a few mol-%.

The thickness of the films may be controlled by watching the interference colours in the reflected white light during the growth of the film. Almost every film was prepared with a thickness of about 1000 Å (corresponding to a white-yellow colour) for mainly two reasons: firstly, it is well known that thick sprayed oxide-films may have a nonuniform structure which may be due to the longer spraying time which leads to a cooling of the substrate so that the final film consists of several subfilms. The subfilms arise because the proportion of Sn, incorporated into the In_2O_3 lattice, strongly depends on temperature; secondly, the position of the plasma resonance maximum (see below) and the frequency ω_p only coincide if $(\omega_p/c)d \ll 1$, c being the velocity of light in vacuum and d the film thickness.

The film thickness was measured interferometrically by Tolansky's method. The Tolansky step was etched using a solution reported by Tarnopol [17] for stripping conductive tinoxide-films from glass.

Conductivity and Hall coefficient were measured in the usual way by compensation. The contacts consisted of a conductive silver paste and were ohmic.

Conductivity and carrier concentration as functions of temperature were measured by means of a He cryostat. The lowest temperature was 16 K.

The aim of the optical measurements was the determination of the complex dielectric constant. The simplest way to get the real and imaginary part of the dielectric constant is to measure the reflectivity and transmissivity for (nearly) normal incidence. The measurements were performed using an monochromator, an integrating sphere [18] and a PbS- or InSb-cell. The transmissivity was measured relative to a fused quartz plate which equals the substrate of the film. Low values of the reflectivity were measured relative to the quartz-substrate, higher ones relative to an evaporated silver-film. The spectral range covered reached from 0.6–4 μ. The real part ε_r and the imaginary part ε_i of the dielectric constant were evaluated simultaneously by an iteration technique which involves the complete Fresnel formulas corrected for the second boundary of the substrate. The measured values of transmissivity and reflectivity were corrected via the optical constants of either Infrasil or silver.

To get a cross check, a further method of determining ε_r and ε_i was used (for wavelength less than 3 μ). The following optical quantities were determined in the range from 0.6–3 μ: 1) Transmissivity and reflectivity for nearly normal incidence, 2) transmissivity for 60° incidence and polarisation (Glan-Thompson prism) parallel to the plane of incidence (*p*-polarisation), 3) transmissivity for 60° incidence and polarisation normal to the plane of incidence (*s*-polarisation), 4) reflectivity for 60° incidence and *p*-polarisation of a silver-coated sample (thereby, light first enters the substrate; the absorptivity is strongly peaked in the vicinity of ω_p, indicating plasma resonance absorption), 5) reflectivity for 60° incidence and s-polarisation of the silver-coated sample, and 6) reflectivity for 30° incidence and *p*-polarisation of the silver coated sample. The iterative least squares method was used to minimize the merit function given by

$$\Phi = [vv], \qquad v_i = F_i(\varepsilon_r, \varepsilon_i) - M_i, \tag{2}$$

where the functions F_i are the appropriate Fresnel-formulas which describe the measured optical quantities (values M_i) mentioned above. This procedure was applied to the samples S 3, S 4, S 5, and S 6.

2. Theory

The theoretical models are given for single-band conduction and noninteracting carriers.

2.1 Mobility for Ionized Impurity Scattering

The well known Brooks-Herring formula [19] for the mobility may be written in the following form for

complete degeneracy [20]

$$\mu = \{3\pi\hbar^3(4\pi\varepsilon_0\varepsilon_g)^2/[4e^3 m_c^2 g(x)]\}(N/N_i), \quad (3)$$

where $x = 0.75(\hbar\omega_p/E_F)^2$ and $g(x) = 0.5[\ln(1+4/x) - 1/(1+x/4)]$. The quantity m_c is the conductivity mass and is identical with the optical mass m_{opt}, N_i is the density of impurity centres. The quantity x is related to the Thomas-Fermi screening length $1/k_{TF}$ by [16]

$$x = (k_{TF}/k_F)^2, \quad (4)$$

where k_F is the Fermi wavenumber given by

$$k_F = (3\pi^2 N)^{1/3} \quad (5)$$

for spherical energy surfaces.
The conductivity is given by [21]

$$\sigma = (Ne^2/m_c) \cdot \tau(E_F), \quad (6)$$

where $\tau(E_F)$ is the relaxation time at the Fermi surface.
Relaxation time and mobility[1] are connected by [21]

$$\mu = (e/m_c) \cdot \tau(E_F) \quad (7)$$

so that

$$\sigma = Ne\mu. \quad (8)$$

If the electron gas is degenerate and the energy surfaces have weak anisotropy and also weak non-parabolicity, N is approximately given by [21]

$$R = 1/(Ne), \quad (9)$$

R being the Hall-coefficient.
Eq. (3) shows that μ and σ are independent of temperature in the degenerate case (where $N \sim E_F^{3/2}$), provided that the impurity density is also independent of temperature. If the carrier density is fairly high, there is a decrease in donor-ionization energy due to the formation of an impurity band [22]. The broadening of the impurity band at increasing carrier concentration leads to an overlapping with the conduction band and the ionization energy of the donors approaches zero. According to Weiher [2] this should already occur with In_2O_3 if the donor-density is as low as 1.5×10^{18} cm^{-3}.

2.2 Plasma Resonance Absorption

The transmission spectrum for p-polarized radiation with oblique incidence of a free-electron-like foil exhibits a more or less sharp minimum (depending on the magnitude of the product $\omega_p\tau$, the film thickness d, and the angle of incidence) in the vicinity of the plasma resonance frequency ω_p [23, 24]. This indicates absorption of radiation. The reason for the absorption is the excitation of plasma modes due to the special geometry of the film, i.e. the two neighbouring film boundaries. The theory of these modes was given by Kliever *et al.* [25, 26] on phenomenological grounds.
The plasma resonance absorption of a semiconducting film is more distinct if the film is deposited on a well-conducting metallic substrate [27, 28, 31]. The position of the maximum of absorption coincides with ω_p provided $\omega_p^2\tau^2 \gg 1$ and $(\omega_p/c)d \ll 1$, so that this important quantity can be measured directly [28]. The plasma resonance absorption can, of course, be treated by means of the common Fresnel formulas.
To measure the plasma resonance absorption, the thin In_2O_3-films were coated with an optically dense Ag-film. Obviously, the radiation must now enter through the Infrasil-substrate. The p-polarisation was achieved by means of a Glan-Thompson prism (for wavelengths less than 2.6 μ) and a gold-wire-grid polarizer (for greater wavelengths).

Besides the transversel modes mentioned above, longitudinal plasma modes exist which show additional absorption peaks for $\hbar\omega > \hbar\omega_p$ [29–34]. A numerical calculation based on the formulas given in [31] showed that these modes are strongly damped in In_2O_3 on account of the short relaxation time. However, it is supposed that the surface roughness with an rms asperity parameter of about 40 Å (Fig. 11) causes the plasma wave to lose phase at random because the wavelength of the plasma wave is comparable with the asperity parameter. So the interference between waves running to and coming from the surface is destructive.

2.3 The Complex Dielectric Constant

According to Spitzer and Fan [35] the real part of the dielectric constant is given by

$$\varepsilon_r = \varepsilon_g[1 - (\omega_p/\omega)^2], \quad (10)$$

provided that $(\omega\tau)^2 \gg 1$. This condition holds fairly well for the In_2O_3-films in the short wavelength region. Thus, ε_r is independent of the scattering mechanism.
The optical mass [see (1)] involves a mean value of the Fermi velocity v over the Fermi surface, and is

[1] In the degenerate case, the Hall mobility is equal to the drift mobility if one assumes a single isotropic band.

given by the relation

$$N/m_{\text{opt}} = \int v \cdot dS_F/(12\pi^3\hbar), \tag{11}$$

where the integration is over the Fermi surface. For isotropic and parabolic energy bands $m_{\text{opt}} = m^*$, where m^* is the standard effective mass.

Extrapolation of ε_r to $\lambda = 0$ yields ε_g, and the zero of ε_r gives the plasma frequency ω_p.

The imaginary part of the dielectric constant, and especially its wavelength dependence, is strongly influenced by the scattering mechanisms. Von Baltz and Escher [16] have given analytical formulas for ε_i for various scattering mechanisms, assuming isotropic and parabolic energy bands, high degeneracy, and negligible broadening of energy levels, i.e. $\omega^2 \cdot \tau^2 \gg 1$.

For photon energies $\hbar\omega \ll E_F$, ε_i exhibits a λ^3 wavelength-dependence, independent of the scattering mechanism, i.e. the familiar Drude formula

$$\varepsilon_i^0 = \varepsilon_g \omega_p^2/[\omega^3 \tau(E_F)] \tag{12}$$

is valid. The scattering mechanism is contained in the relaxation time.

Numerical evaluation of the analytical formulas shows that the condition $\hbar\omega \ll E_F$ can be replaced by $\hbar\omega < E_F$ [16]. For the range $\hbar\omega \gg E_F$, one can rewrite the expressions for ε_i of von Baltz and Escher [16] for ionized impurity scattering, by introducing the relaxation time which follows from (7) and (3). The result is

$$\varepsilon_i^{\infty} = (4/3)(E_F/\hbar)^{1.5} \cdot [1/g(x)] \cdot \varepsilon_g \cdot \omega_p^2/[\omega^{4.5} \tau(E_F)]. \tag{13}$$

However, this result is only a poor approximation for $\hbar\omega \gtrsim E_F$. For this energy range one must return to the exact analytical expression. This was done and the result is shown in Fig. 1 for a hypothetical In_2O_3-film with $\lambda_p = 2\pi c/\omega_p = 1.8\,\mu$, and $\hbar\omega_p = E_F = 0.69$ eV, so that $x = 0.75$ [see (3)]. For comparison, the formulas for other scattering mechanisms have also been evaluated[2].

It is seen from the curve for ionized impurity scattering in Fig. 1 that the wavelength dependence is approximately λ^4 for $\hbar\omega > E_F$ rather than $\lambda^{4.5}$, as expressed by (13). Of course, the power-law is dependent on the quantity x.

On account of the approximate λ^4-law, it should be possible to express ε_i by the following proportionality

$$\varepsilon_i \sim (E_F/\hbar) \cdot [1/g(x)] \cdot \varepsilon_g \cdot \omega_p^2/[\omega^4 \cdot \tau(E_F)]. \tag{14}$$

Assuming $E_F \sim N^{2/3}$, it follows from (14) and (1) that

$$\varepsilon_i \cdot \tau(E_F) \cdot g(x) \sim N^{5/3}, \quad \omega = \text{const.} \tag{15}$$

3. Experimental Results and Interpretation

The temperature dependence of the carrier concentration indicates degeneracy of the electron gas. The constant values of the conductivity and the mobility at low temperatures points to a scattering mechanism independent of temperature, like impurity scattering.

Assuming now that ionized impurity scattering is the predominant scattering mechanism, (3) should

[2] The reader is refered to Ref. [16].

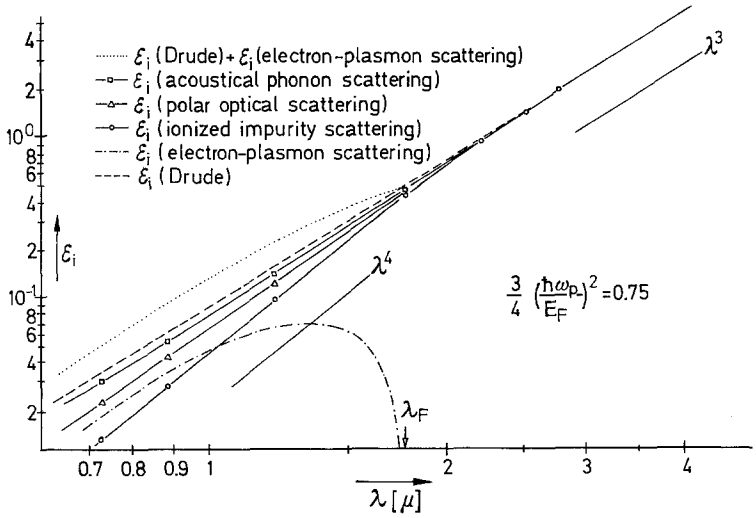

Fig. 1. Imaginary part ε_i of the dielectric constant for various scattering mechanisms as a function of the wavelength λ for a hypothetical In_2O_3-film. Plasma wavelength $\lambda_p = 1.8\,\mu$, Fermi energy $E_F = 0.69$ eV, plasmon energy $\hbar\omega_p = 0.69$ eV

Table 1

Sample	d[Å]	$N[10^{20}\,cm^{-3}]$	$\lambda_p[\mu]$	$\lambda_F = 1.24/E_F[\mu]$	$[\omega_p\tau(E_F)]^{-1}_{opt}$	$[\omega_p\tau(E_F)]^{-1}_{stat}$	$\mu[cm^2/Vs]$	N/N_i
S1	2080	0.87	3.47	4.96	0.34	0.45	24.8	0.6
S2	980	1.86	2.65	3.02	0.26	0.28	30.8	0.8
S3	920	2.08	2.49	2.82	0.18	0.17	47.0	1.2
S4	960	3.12	2.07	2.21	0.17	0.15	43.7	1.2
S5	940	3.87	1.91	2.03	0.15	0.18	31.0	0.9
S6	890	4.22	1.85	1.94	0.13	0.14	38.8	1.1
S7	956	4.44	1.83	1.94	0.13	0.11	48.0	1.3
S8	921	4.57	1.78	1.88	0.13	0.13	39.8	1.1
S9	889	0.75	4.06	5.64	–	–	46.1	0.8
S10	952	1.13	3.53	4.28	–	–	32.8	0.7
S11	875	1.26	3.22	3.88	–	–	42.6	0.9
S12	964	1.96	2.52	2.95	–	–	24.8	0.6
S13	2230	2.04	2.50	2.82	0.27	0.46	17.4	0.8

d = film thickness; N = carrier concentration; λ_p = plasma wavelength; ω_p = plasma frequency; λ_F = Fermi wavelength; E_F = Fermi energy; μ = mobility; $\tau(E_F)$ = relaxation time at the Fermi energy; N_i = concentration of ionized impurities.

be adequate to describe the measured mobility-values. However, it may be argued that the poly-cristalline structure of the films (see Figs. 9 and 10) may give false results for the mobility measured statically. Nevertheless, the agreement of the statical and optical relaxation time (see Table 1) indicates that barrier resistivities at the grain boundaries are not present in In_2O_3-films. Thus the mobility determined statically should be the mobility within the cristallites.

If one calculates the quotient N/N_i using (3) and assumes that the Fermi energy is given by

$$E_F = [\hbar^2/(2m_d)] \cdot (3\pi^2 N)^{2/3} \tag{16}$$

with the density-of-states mass m_d equal to the optical mass m_{opt}[3], the values given in Table 1 are obtained[4]. They show that $N \approx N_i$, as was to be expected. It is well known that (3) overestimates the scattering cross section so that in reality the values N/N_i are less than those deduced from (3). The tendency of the quotient N/N_i to values less than one may possibly be explained by partial compensation of the donors by acceptors.

The real part of the dielectric constant of films of different electron concentration is shown in Fig. 2. In the short wavelength region ($\omega^2\tau^2 \gg 1$), ε_r exhibits a linear dependence on λ^2 in accordance with (10). Towards longer wavelengths, the deviation from the quadratic law is due to the decrease of $\omega\tau$. Extrapolation to $\lambda = 0$ leads to $\varepsilon_g = 4$, a value virtually independent of the carrier concentration. The intersections of the curves with the line $\varepsilon_r = 0$ yield the plasma resonance frequencies.

The imaginary part of the dielectric constant exhibits a linear dependence on λ^3 for longer wave-

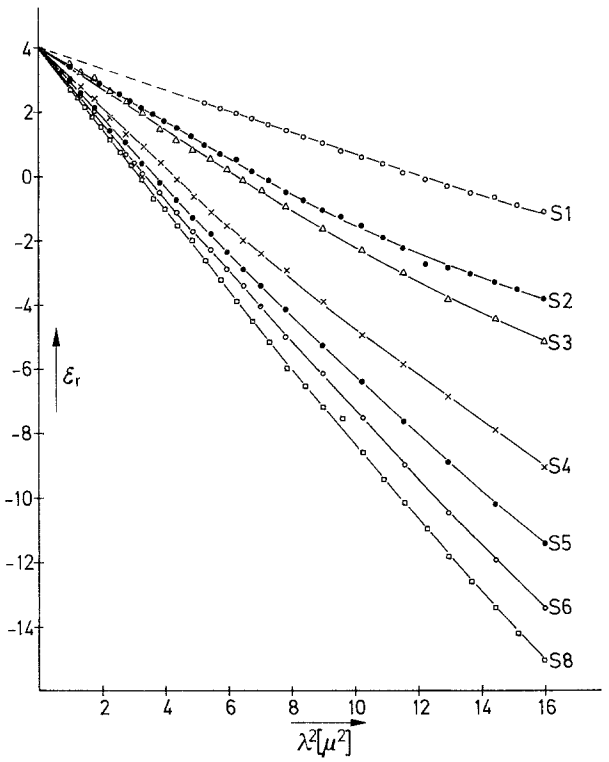

Fig. 2. Real part ε_r of the dielectric constant as a function of the square of the wavelength λ for the several In_2O_3-films S1–S6 and S8

[3] The reason for setting $m_d = m_{opt}$ is given later.

[4] For samples S1 and S13 τ_{opt} was used to calculate N/N_i.

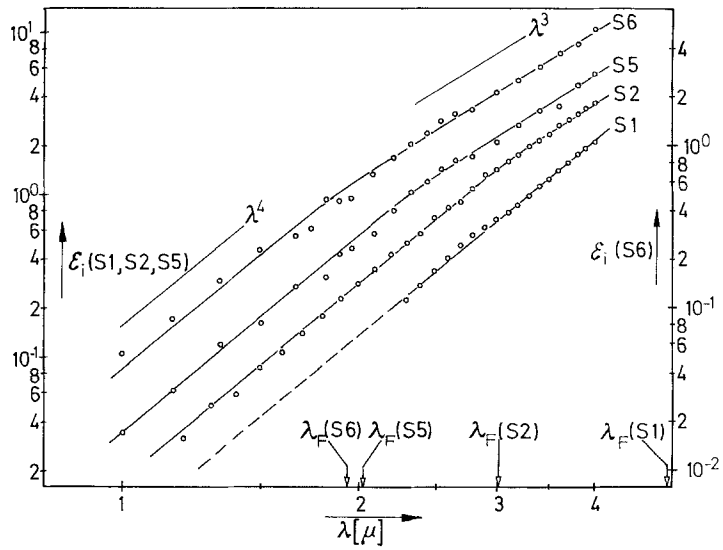

Fig. 3. Imaginary part ε_i of the dielectric constant as a function of the wavelength λ for several In_2O_3-films (S1, 2, 5 and 6) with Fermi-wavelength λ_F

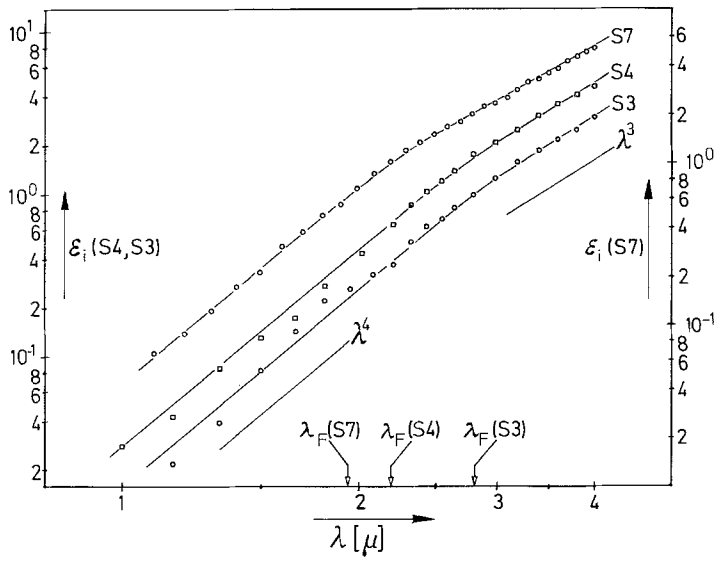

Fig. 4. Imaginary part ε_i of the dielectric constant as a function of the wavelength λ for several In_2O_3-films (S3, 4 and 7) with Fermi wavelength λ_F

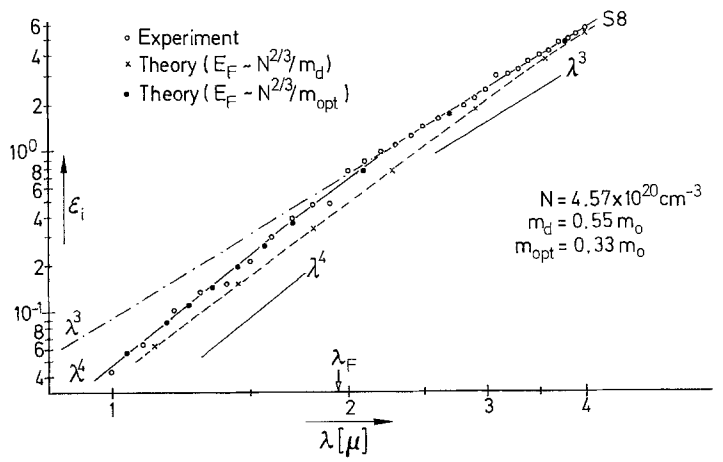

Fig. 5. Comparison between experiment and theory. Theoretical points (●, ×): imaginary part ε_i of the dielectric constant as a function of the wavelength λ, calculated for ionized impurity scattering (the Fermi energy E_F was computed using the optical mass $m_{opt} = 0.33$, electron masses m_0, and the density-of-states mass $m_d = 0.55\ m_0$, respectively). Experimental points (○): imaginary part ε_i of the dielectric constant for sample S8 with Fermi wavelength λ_F calculated using m_{opt}

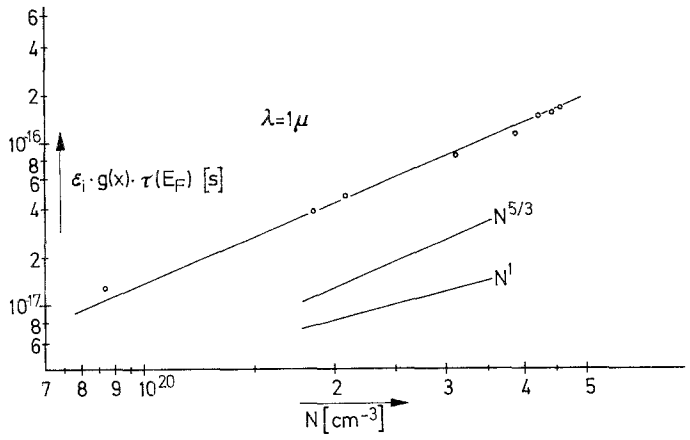

Fig. 6. Reduced imaginary part $\varepsilon_i \cdot \tau(E_F) \cdot g(x)$ of the dielectric constant at the given wavelength $\lambda = 1\,\mu$ as a function of the electron concentration N. $\tau(E_F)$ is the relaxation time at the Fermi energy $E_F(x = 0.75(\hbar\omega_p/E_F)^2$ with plasmon energy $\hbar\omega_p$, $g(x) = 0.5[\ln(1 + 4/x) - (1 + x/4)^{-1}]$)

lengths, as can be seen from Figs. 3 through 5. The slopes of the ε_i versus λ^3-lines give the optically relevant relaxation times of the various films and may be compared with the statical relaxation times. The dimensionless quantities $1/[\omega_p \cdot \tau(E_F)]$ are listed in Table 1. One sees that the optical and statical values agree fairly well for thin films. The thicker films (S1 and S13) show a discrepancy between τ_{opt} and τ_{stat} which may be due to barrier effects, but also to inhomogeneity.

Furthermore, Figs. 3 through 5 show that the λ^3-law is valid up to $\hbar\omega \approx E_F$, in accordance with theory. For wavelengths smaller than the Fermi wavelength λ_F, defined by $\lambda_F = 2\pi c\hbar/E_F$, the lines have a greater slope representing an approximate λ^4-law for all films[5]. The bend-over occurs in the vicinity of $\hbar\omega = E_F$, E_F being calculated by means of (16). This behavior is indicated by theory (see Fig. 1). None of the other scattering mechanisms can account for the λ^4-law.

Figure 3 shows a quantitative comparison between theory and experiment assuming ionized impurity scattering to be the predominant scattering mechanism. The theoretical curve is fitted to the experimental λ^3-law for $\hbar\omega < E_F$. The agreement is satisfactory, above all, the bend-over is reproduced. If one tries to calculate E_F using the density-of-states mass $m_d = 0.55$ determined by Weiher and Dick [4] and also by Vainshtein and Fistul' [14], the theoretical and experimental curves disagree. The bend-over occurs now at a longer wavelength and the λ^4-law is not reproduced.

According to (15), the term $\varepsilon_i \cdot \tau(E_F)g(x)$ should be proportional to $N^{5/3}$ at a constant wavelength. Figure 6 shows the experimental result, where λ was choosen to be 1 μ. The experimental slope agrees with that predicted by theory.

To determine the optical mass, the positions ω_p of the maxima of the plasma peaks (Fig. 7) and the

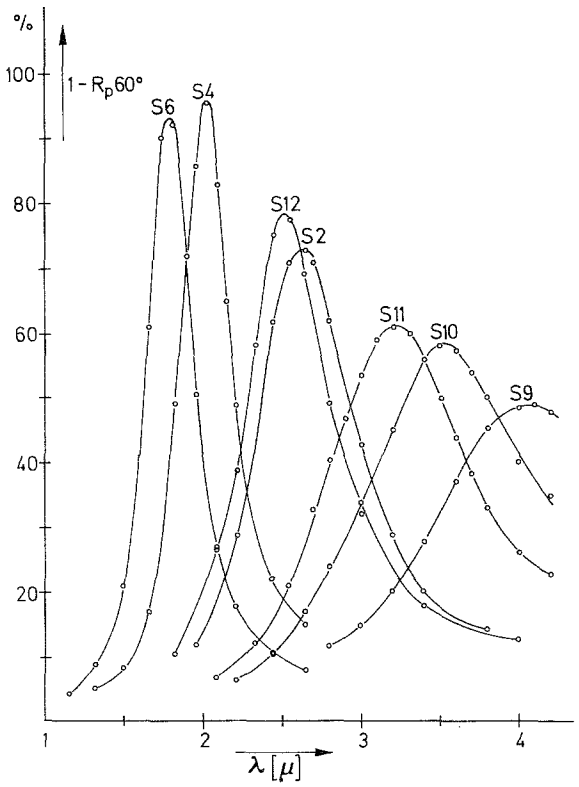

Fig. 7. Optical plasma resonance absorption $A_p = 1\text{-}R_p$ as a function of the wavelength λ for several In_2O_3-films (S2, 4, 6 and 9–12). R_p is the value of the reflectivity of p-polarized radiation with angel of incidence $\Theta = 60°$ relative to a silver standard. The films on Infrasil were coated with silver and the radiation entered through the substrate

[5] The same law was found by Müller [7].

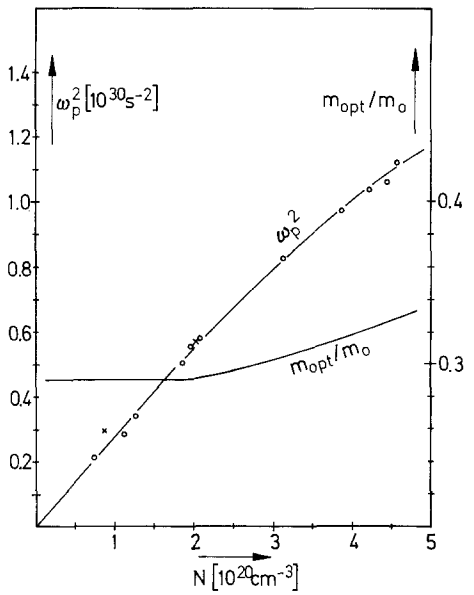

Fig. 8. Square of the plasma resonance frequency ω_p and optical mass m_{opt} normalized to the electron mass m_0 as functions of the electron concentration N

values of ω_p obtained from the zeros of the different curves for ε_r in Fig. 2 were plotted as a function of N (Fig. 8). If the ω_p^2 versus N-curve were linear, the optical mass would be constant. However, the measurements indicate that the optical mass depends slightly on carrier concentration in contrast to the results of Vainshtein and Fistul' [14] who found the constant value 0.28 for m_{opt}/m_0, m_0 being the free electron mass. The experimental error of m_{opt} is less than 10% so that the increase of m_{opt} is a real effect which may be due to both non-parabolicity and increasing proportion of Sn incorporated in the In_2O_3-lattice.

4. Film Structure

Scattering at grain boundaries may also influence the electrical and optical properties of polycristalline films. The value of the relaxation time for this scattering process may be estimated by [36]

$$\tau = L/v_F, \tag{17}$$

where L is an average crystallite size, and v_F the Fermi velocity.

The structural investigations were performed by means of an electron microscope. The films ($d \approx 400$–600 Å) were prepared on NaCl and Ca-aluminate glass. It is supposed that the film structure on Ca-aluminate glass is similar to that on fused quartz. The films on Ca-aluminate could be loosened by a treatment with HNO_3. Stripping the films from quartz was not possible. The electron-micrographs are shown in Figs. 9 and 10. The average crystallite size is about 400 Å. For comparison, a Pt-C replica (45°) of a 900 Å thick film is shown in Fig. 11. The average lateral dimension of the surface roughness agrees with the average crystallite size in Figs. 9 and 10. As can be deduced from the data of Table 1, the mean free path measured is about 50 Å. Hence, it

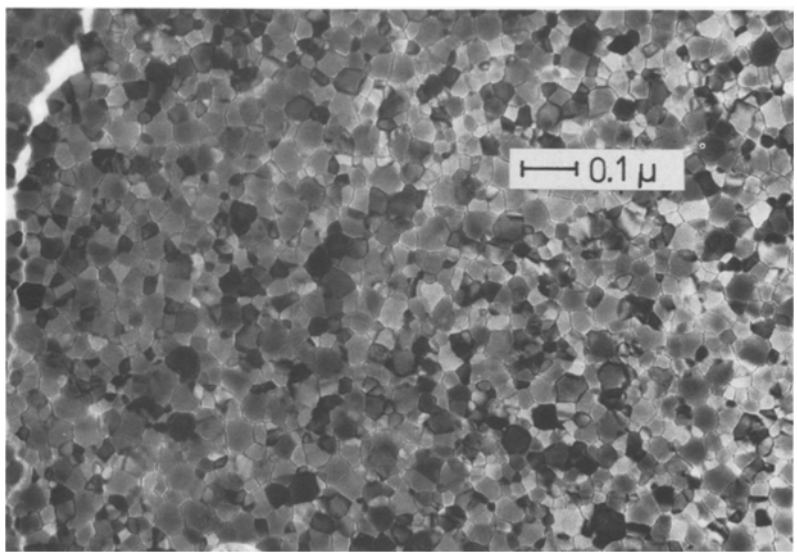

Fig. 9. Electron micrograph of an In_2O_3-film (similar to sample S6) on NaCl. The film thickness is about 400–600 Å

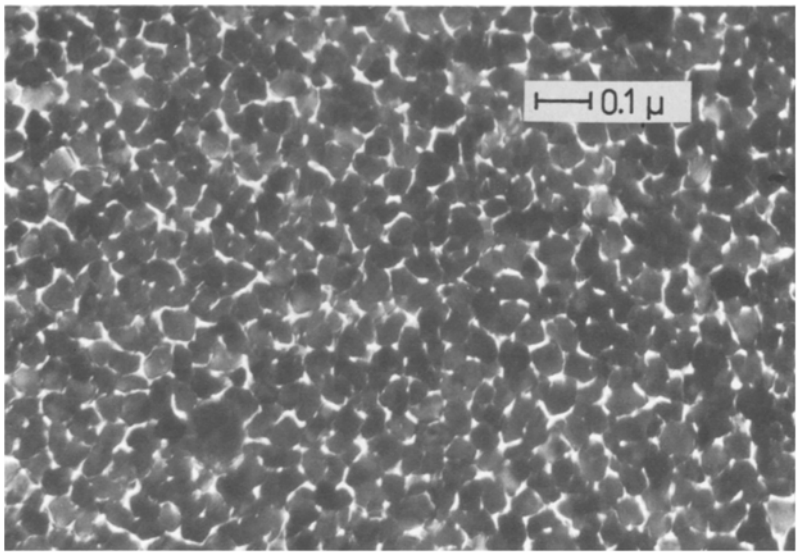

Fig. 10. Electron micrograph of an In_2O_3-film (similar to sample S8) on Ca-aluminate glass. The film thickness is about 400–600 Å

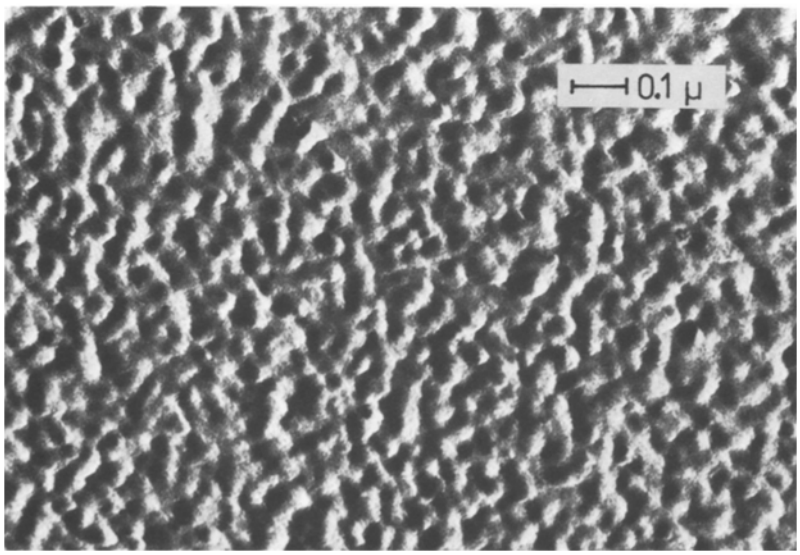

Fig. 11. Pt-C replica of an In_2O_3-film (similar to sample S2) on Infrasil. The film thickness is about 900 Å

may be concluded that grain boundary scattering does not affect the electrical and optical properties of the films decisively.

Acknowledgements. The author would like to thank Prof. Dr. C. von Fragstein for valuable comments and the possibility to carry through this work, Prof. Dr. G. Schulz and Dipl.-Phys. J. Gutjahr for helpful discussions, and Dipl.-Phys. E. Fries for many suggestions concerning the experiments.

References

1. G. Rupprecht: Z. Physik **139**, 504 (1954)
2. R. L. Weiher: J. Appl. Phys. **33**, 2834 (1962)
3. R. L. Weiher, R. P. Ley: J. Appl. Phys. **37**, 299 (1966)
4. R. L. Weiher, B. G. Dick, Jr.: J. Appl. Phys. **35**, 3511 (1964)
5. R. Groth: Phys. Stat. Sol. **14**, 69 (1966)
6. H. K. Müller: Phys. Stat. Sol. **27**, 723 (1968)
7. H. K. Müller: Phys. Stat. Sol. **27**, 733 (1968)
8. V. F. Korzo, L. A. Ryabova: Sov. Phys.-Solid State **9**, 745 (1967)
9. J. L. Vossen: RCA Rev. **32**, 289 (1971)
10. D. B. Fraser, H. D. Cook: J. Electrochem. Soc. **119**, 1368 (1972)
11. L. I. Burbulyavicus, V. M. Vainshtein, L. G. Gerasimova, M. N. Danchevskaya, S. V. Khrustaleva: Izv. Akad. Nauk SSSR, Neorg. Mater. **5**, 551 (1969)
12. V. A. Williams: J. Electrochem. Soc. **113**, 234 (1966)
13. V. I. Fistul', V. M. Vainshtein: Sov. Phys.-Solid State **8**, 2769 (1967)

14. V. M. Vainshtein, V. I. Fistul': Sov. Phys.-Semicond. **1**, 104 (1967)
15. V. M. Vainshtein, V. I. Fistul': Sov. Phys.-Semicond. **4**, 1495 (1970)
16. R. von Baltz, W. Escher: Phys. Stat. Sol. (B) **51**, 499 (1972)
17. R. S. Tarnopol: Chem. Abst. **46**, 11616i (1952)
18. J. C. Morris: Appl. Optics **5**, 1036 (1966)
19. H. Brooks: Phys. Rev. **83**, 879 (1951)
20. R. B. Dingle: Phil. Mag. **46**, 831 (1955)
21. F. J. Blatt: In *Solid State Physics*, Vol. 4 (Academic Press, New York 1957) pp. 199–366
22. G. L. Pearson, J. Bardeen: Phys. Rev. **75**, 865 (1949)
23. A. J. McAllister, E. A. Stern: Phys. Rev. **132**, 1599 (1963)
24. M. Hattori, K. Yamada, H. Suzuki: J. Phys. Soc. Japan **18**, 203, (1963)
25. R. Fuchs, K. L. Kliever, W. J. Pardee: Phys. Rev. **150**, 589 (1966)
26. K. L. Kliever, R. Fuchs: Phys. Rev. **153**, 498 (1967)
27. R. W. Berreman: Phys. Rev. **130**, 2193 (1963)
28. M. Bischoff, H. Finkenrath, W. Waidelich: Z. Physik **231**, 193 (1970)
29. R. Melnyk, M. J. Harrison: Phys. Rev. Letters **21**, 85 (1968)
30. R. Melnyk: Phys. Rev. B **2**, 835 (1970)
31. R. Clanget: Optik **35**, 180 (1972)
32. W. E. Jones, K. L. Kliever, R. Fuchs: Phys. Rev. **178**, 120 (1969)
33. I. Lindau, P. O. Nilsson: Phys. Letters **31** A, 352 (1970)
34. M. Anderegg, B. Feuerbacher, B. Fitton: Phys. Rev. Letters **27**, 1565 (1971)
35. W. G. Spitzer, H. Y. Fan: Phys. Rev. **106**, 882 (1957)
36. R. Grigorovici, G. Ciobanu: *Basic Problems in Thin Film Physics* (Vandenhoeck & Ruprecht, Göttingen 1966) pp. 596–600